Charge ordering geometries in uniaxially strained NbSe₂

Felix Flicker[*]

Department of Physics, University of California, Berkeley, California 94720, USA

Jasper van Wezel[†]

Institute for Theoretical Physics, University of Amsterdam, 1090 GL Amsterdam, The Netherlands

Recent scanning tunneling microscopy experiments reveal niobium diselenide to support domains of striped ($1Q$) charge order side by side with its better-known triangular ($3Q$) phase, suggesting that small variations in local strain may induce a quantum phase transition between the two. We use a theoretical model of the charge order in NbSe₂, based on a strong momentum- and orbital-dependent electron-phonon coupling, to study the effect of uniaxial strain. We find that as little as 0.1% anisotropic shift in phonon energies breaks the threefold symmetry in favor of a $1Q$ state, in agreement with the experimental results. The altered symmetries change the transition into the ordered state from weakly first order in the $3Q$ case to second order in the $1Q$ regime. Modeling the pseudogap phase of NbSe₂ as the range of temperatures above the onset of long-range order in which phase coherence is destroyed by local phonon fluctuations, we find a shortening of the local ordering wave vector with increasing temperature, complementing recent x-ray diffraction observations within the low-temperature phase.

PACS number(s): 71.45.Lr

*The stability of different charge density wave (CDW) geometries is a topic of much current interest. In the simplest case a "$1Q$" CDW selects a single preferential direction [1]. In two-dimensional materials, two perpendicular $1Q$ CDWs can coexist, creating a $2Q$ pattern. In layered high-temperature superconductors such a checkerboard state is believed to compete with $1Q$ order [2–5]; recently the $1Q$ state was found to dominate the $2Q$ in YBa₂Cu₃O₇ (YBCO) [6]. The layered hexagonal structure of niobium diselenide ($2H$-NbSe₂) allows instead for a $3Q$ triangular CDW with three superposed $1Q$ patterns [7–10]. Recent surface studies via scanning tunneling microscopy (STM) suggest a quantum phase transition between $3Q$ and $1Q$ states in NbSe₂ may be tuned by local strain, offering the possibility of studying the interplay between the two, as well as a direct comparison to the high-T_c case [11,12].

It was recently shown that the minimal model reproducing the full range of experimental observations on the $3Q$ ordered state in NbSe₂ includes a strong electron-phonon coupling, dependent on both the momenta and the orbital characters of the electronic states scattered between [13]. Motivated by the recent STM observations, in this Rapid Communication we employ the same model in a free energy analysis to study the charge-ordered state upon application of uniaxial strain [12]. We find that while the $3Q$ state, which respects the threefold lattice symmetry, is the lowest-energy configuration in the unstrained case, little uniaxial strain is required to break the symmetry to $1Q$, agreeing with suggestions that lattice defects may locally stabilize the $1Q$ state [12]. We find that the $1Q$ phase transitions are second order, whereas the $3Q$ transitions are weakly first order. With increasing temperature we predict a shortening CDW wave vector in the locally fluctuating, short-range-ordered, pseudogap regime above the CDW transition, analogous to the recently observed nonmonotonic evolution of the CDW wave vector within the ordered state [14].

_____

[*]flicker@physics.org
[†]vanwezel@uva.nl

Model. Niobium diselenide consists of hexagonal layers of niobium atoms sandwiched between layers of selenium atoms, displaced so that they lie above and below half of the Nb interstitial locations. The crystal structure and band structure are depicted in Fig. 1. Consecutive sandwich layers are displaced to have the complementary half of the interstices occupied, giving two formula units per unit cell. $3Q$ charge order develops below 33.5 K. Recent STM measurements show stable domains of $1Q$ order on the surface of NbSe₂, coexisting with neighboring regions of $3Q$ order, and occurring in areas where the topmost niobium layer is slightly raised [12]. This suggests that the $1Q$ state may be stabilized by local strain, causing a quantum phase transition between the $1Q$- and $3Q$-ordered states [12]. The CDW wave vector $\mathbf{Q}_{\text{CDW}} = (1 - \delta)\frac{2}{3}\Gamma M$ is found to be incommensurate with the lattice in both geometries, with $\delta_{3Q} \approx 0.014$ and $\delta_{1Q} \approx 0.143$ [7,12].

It has previously been shown that the CDW transition in NbSe₂ can be successfully described by a strong coupling between electrons ψ and atomic displacements φ through the interaction [13]

$$\hat{H}_{\text{int}} = \sum_{\mu\nu\mathbf{k}\mathbf{q}} \mathbf{g}^{\mu,\nu}_{\mathbf{k},\mathbf{k}+\mathbf{q}} \hat{\varphi}^{\dagger}_{\mathbf{q}} \hat{\psi}^{\nu\dagger}_{\mathbf{k}} \hat{\psi}^{\mu}_{\mathbf{k}+\mathbf{q}}, \qquad (1)$$

where the electron-phonon coupling $\mathbf{g}^{\mu,\nu}_{\mathbf{k},\mathbf{k}+\mathbf{q}}$ depends on the momenta of both the ingoing and outgoing electron states and the bands μ, ν scattered between. The analytic expression for $\mathbf{g}$ has been shown to be applicable to a range of transition metal compounds including NbSe₂, and accounts for the orbital characters of the electron bands with dispersion $\xi^{\mu}_{\mathbf{k}}$ crossing the Fermi level [13,17]. It yields a stronger electron-phonon coupling in the lower band than the upper, explaining the order-of-magnitude difference in CDW gap size of the two bands in angle-resolved photoemission spectroscopy (ARPES) [13,18,19]. We restrict attention to the lowest band from here on. This model reproduces the full host of available experimental observations on the $3Q$ state, with the overall

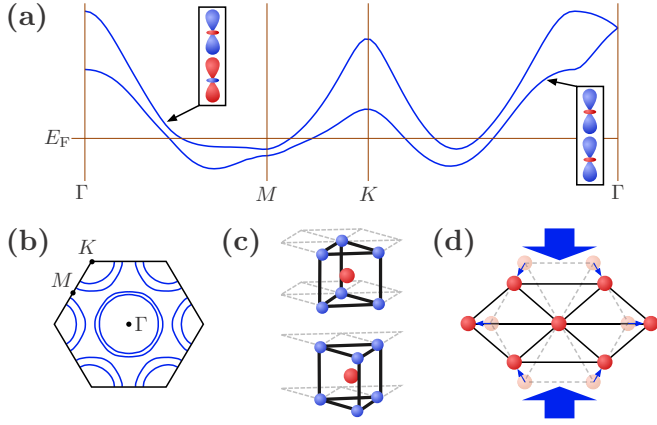**(a)**

(b) **(c)** **(d)**

FIG. 1. (Color online) (a) The band structure of NbSe$_2$ modeled by the tight-binding fit described in Ref. [13]. Only the bands crossing E_F are shown, corresponding primarily to bonding and antibonding combinations of the two niobium $d_{3z^2-r^2}$ orbitals within a unit cell. Only the lower band is involved in the CDW formation. (b) The Fermi surface consists of concentric barrel-shaped pockets around the Γ and K points [8,13,15,16]. We ignore a small pocket around Γ. (c) The layered structure of NbSe$_2$, with Nb in red and Se in blue. (d) The atomic displacements of the crystal structure caused by uniaxial strain within the plane of Nb atoms, indicated by the large blue arrows. Keeping the volume of the unit cell constant and increasing the horizontal interatomic distances to $x_0 + \epsilon$ causes the diagonal interatomic distances to become approximately $x_0 - \epsilon/2$.

strength of the electron-phonon coupling as the only free parameter (chosen to give the observed transition temperature of 33.5 K) [13].

Following Ref. [10], we model the (isotropic) bare phonon dispersion $\Omega_0(|\mathbf{q}|)$ by a Brillouin function with a maximum of 11.2 meV at the zone boundary. Since the longitudinal phonon is seen to soften in inelastic x-ray scattering [10], we restrict our attention to $g = \hat{\mathbf{q}} \cdot \mathbf{g}$. Uniaxial strain is modeled as an anisotropic linear shift in bare phonon frequencies. As shown in Fig. 1(d), stretching the lattice in one direction causes a contraction in the perpendicular direction. We correspondingly define a strain parameter σ through $\Omega_1 = \Omega_0(1 + \sigma)$ along one of the $\mathbf{Q}_{CDW} \parallel \Gamma M$ directions, and $\Omega_{2,3} = \Omega_0(1 - \frac{\sigma}{2})$ in the $2\pi/3$-rotated directions.

Landau theory. The free energy can be expanded in terms of the three order parameters $\varphi_j = \langle \hat{\varphi}(\mathbf{q}_j) \rangle$, where $\mathbf{q}_j = (1 - \delta)\frac{2}{3}\Gamma M_j$, and j labels the three inequivalent ΓM directions. At any given value for δ, the most general free energy to fourth order in φ_j is

$$\beta F[\varphi_1, \varphi_2, \varphi_3] = -\sum_{j=1}^{3}\{a(\Omega_j)|\varphi_j|^2\} - b\varphi_1\varphi_2\varphi_3$$
$$+ c\sum_{j \bmod 3}\{|\varphi_j|^4 + d|\varphi_j|^2|\varphi_{j+1}|^2\}. \quad (2)$$

The phases of φ_j are chosen such that the third-order term is real and b is positive. Starting from the Hamiltonian of Eq. (1), the coefficients a–d, and their dependences on $\mathbf{q}$ and $\beta = 1/T$, can be evaluated numerically [3]. Strain enters via the Ω_j dependence of the quadratic coefficient.

In the $3Q$ phase the order parameters obey $\varphi_1 = \varphi_2 = \varphi_3 \equiv \varphi$, while in each of the $1Q$ phases only a single φ_j is nonzero. The free energy then takes the forms

$$\beta F_{1Q}^j[\varphi_j] = -a(\mathbf{q}_j, T, \Omega_j)|\varphi_j|^2 + c(\mathbf{q}_j, T)|\varphi_j|^4,$$

$$\beta F_{3Q}[\varphi] = -\sum_{j=1}^{3} a(\mathbf{q}_j, T, \Omega_j)|\varphi|^2 - b(\mathbf{q}, T)\varphi^3$$
$$+ 3c(\mathbf{q}, T)[1 + d(\mathbf{q}, T)]|\varphi|^4, \quad (3)$$

where b–d do not depend on strain, and can be evaluated along any of the ΓM directions. The boundedness of the free energy requires $c > 0$, which is the case in all calculations described below.

Starting from a disordered state with $a < 0$, minimization of Eq. (3) yields a second-order phase transition into either a $3Q$ or a $1Q$ state whenever a becomes positive. If a stays negative, but $c(1 + d) < -\frac{b^2}{18a}$, a $3Q$ state forms via a first-order transition. Both scenarios require $d > -1$, which is the case for all calculations considered. For any nonzero b, approaching a second-order transition into the $3Q$ state at $a = 0$ causes a divergence in b^2/a, which forces a first-order transition into the $3Q$ state instead. The two (would-be) transitions are typically close in temperature and strain, suggesting a weakly first-order transition [20]. We therefore only expect either a second-order transition from disorder into a $1Q$ state, or a first- or weakly first-order transition from disorder into the $3Q$ state.

Temperature dependence. The quadratic coefficient in Eq. (3) describes the electronic susceptibility towards the formation of charge order, given by

$$a(\mathbf{q}_j, T, \Omega_j) = -\Omega_j(\mathbf{q}_j) + \chi(\mathbf{q}_j, T),$$
$$\chi(\mathbf{q}_j, T) = -\sum_{\mathbf{k}} |g_{\mathbf{k}, \mathbf{k}-\mathbf{q}}|^2 \text{Re}\left[\frac{f(\xi_{\mathbf{k}}) - f(\xi_{\mathbf{k}-\mathbf{q}})}{\xi_{\mathbf{k}} - \xi_{\mathbf{k}-\mathbf{q}} - i\delta}\right], \quad (4)$$

where $f(\xi_{\mathbf{k}})$ is the Fermi-Dirac distribution, and $\delta \to 0^+$. The definition of the "generalized susceptibility" χ follows Refs. [13,16,21], and is expressed here within the random phase approximation (RPA). The usual (bare electronic) susceptibility $\chi_0(\mathbf{q}, T)$ is given by χ with g set to unity. Note that $\sum_j a(\mathbf{q}_j, T, \Omega_j)$, appearing in F_{3Q}, is independent of strain. CDW order first sets in when a changes sign, meaning χ has renormalized the phonon to zero energy at a nonzero wave vector $\mathbf{q} = \mathbf{Q}_{CDW}$. At zero strain, $\mathbf{Q}_{CDW}$ within RPA agrees with the experimentally observed CDW wave vector [13].

To properly account for the system's temperature dependence, it is necessary to include the entropy of the phonon field [22] by introducing internal phonon lines into the RPA diagrams [23–25]. To fourth order in the coupling g, two such terms contribute to χ, shown in Fig. 2. Their self-consistent inclusion forms the mode-mode coupling approximation (MMA), known to give more accurate temperature dependences than RPA in a range of transition metal compounds [23–25]. We neglect one of the diagrams by appeal to Migdal's theorem, since it contains only a vertex correction. The remaining diagram, constituting a self-energy correction to the electrons, is responsible for the observed suppression of the RPA transition temperature in NbSe$_2$ [13].
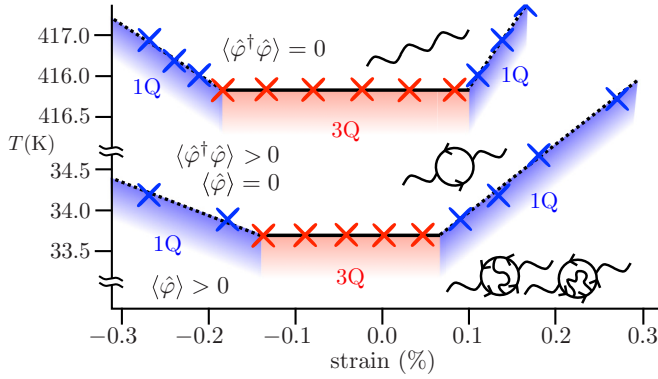
FIG. 2. (Color online) The phase diagram of NbSe$_2$ as a function of uniaxial strain and temperature. Cooling from high temperature, the disordered system develops fluctuating short-ranged order when the RPA predicts a transition, but long-range phase coherence is suppressed by phonon fluctuations in the MMA. As the system cools further, long-ranged CDW order sets in at T_{MMA}. The order changes from $3Q$ to $1Q$ at an anisotropy in phonon energy of about 0.1%. Dashed black lines indicate second-order phase transitions, whereas solid black lines indicate weakly first-order transitions.

The range of temperatures in which RPA predicts order, while MMA predicts the order to be suppressed by the entropy of the phonon field, can be interpreted as a pseudogap regime [13]. In this regime the local amplitude of the displacements, $\sqrt{\langle \hat{\varphi}^\dagger \hat{\varphi} \rangle}$, is nonzero, while the order parameter itself, $\langle \hat{\varphi} \rangle$, averages to zero through fluctuations in phase [24–26]. The result is fluctuating short-range order without long-range phase coherence [27].

The CDW wave vector. Numerically evaluating the coefficients in Eq. (3), within RPA, yields a weakly first-order phase transition from a high-temperature disordered state to a $3Q$ CDW at $T_{RPA} = 416$ K. Including phonon fluctuations via MMA suppresses the order, resulting in fluctuating regions of $3Q$ order without long-range coherence. At $T_{MMA} = 33.5$ K we find a weakly first-order transition in MMA, again to a $3Q$ state. This is interpreted as the onset of long-range phase coherence [27], as indicated in Fig. 2.

The CDW wave vector $\mathbf{Q}_{CDW}$ coincides with the maximum of the quadratic coefficient $a(\mathbf{q}_j)$ in the free energy, or, equivalently, of the generalized susceptibility χ of Eq. (4). The shape of χ is a convolution of the squared electron-phonon coupling with the bare electronic susceptibility χ_0. The CDW wave vector is selected either by a divergence in χ_0 due to Fermi surface nesting, by a strongly peaked dependence of the electron-phonon coupling on electron momenta, or by a combination of the two; in NbSe$_2$, $\mathbf{Q}_{CDW}$ is selected predominantly by the wave-vector dependence of g [9,13].

While the MMA free energy expansion is strictly valid only close to the transition temperature, the susceptibility can still be evaluated within the same approximation at temperatures above T_{MMA}. Similarly, the RPA expansion is valid only slightly above T_{RPA}, but the susceptibility can still be evaluated within the RPA-ordered regime. The peaks of χ within these approximations provide an estimate for the CDW wave vector within the locally fluctuating short-range-ordered region characterizing the pseudogap regime. As temperature
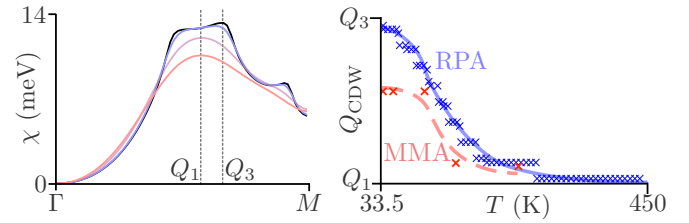

FIG. 3. (Color online) Left: The (strain-independent) generalized susceptibility χ along ΓM in the RPA. From top to bottom, the black curve is at 33.5 K, blue 100 K, purple 303.5 K, and red 500 K. The experimentally observed CDW wave vectors for the two geometries, Q_1 and Q_3, are indicated. Right: The peak position of χ, which dictates the CDW ordering vector within the fluctuating, short-range-ordered regions, decreases with increasing temperature. Both the results of the MMA and RPA calculations are indicated; jumps are numerical artefacts. The solid and dashed lines are guides to the eye only.

increases, $\chi_0(\mathbf{q}_j)$ broadens, and peaks in the temperature-independent electron-phonon coupling begin to dominate χ. The result is a decrease in the local $|\mathbf{Q}_{CDW}|$ as temperature increases in the range $T_{MMA} < T < T_{RPA}$, shown in Fig. 3. A crossover between two distinct regimes, one close to T_{MMA} and the other at high temperatures, can clearly be seen. In the former regime, the bare susceptibility can modify the detailed momentum dependence of the electron-phonon coupling and cause small local extrema to appear in the full susceptibility, thus setting the precise value of $\mathbf{Q}_{CDW}$ at low temperatures. Beyond the crossover, temperature has smoothed these local extrema, and the CDW wave vector is determined solely by the remaining momentum dependence of the electron-phonon coupling. This evolution complements recent x-ray diffraction observations within the ordered phase, of a nonmonotonic evolution of $\mathbf{Q}_{CDW}$ as temperature increases towards T_{CDW} from below [14].

Phase diagram. Tracking the coefficients of the free energy as functions of uniaxial strain and temperature yields the phase diagram of Fig. 2. The range of temperatures between T_{RPA} and T_{MMA} again corresponds to a pseudogap regime characterized by fluctuating local order [13,27]. Starting from unstrained conditions, it takes of order 0.1% anisotropic change in the bare phonon energy to break the $3Q$ symmetry to $1Q$. To estimate the corresponding lattice deformations, we use the in-plane Grüneisen parameter $-(a/\Omega_0)d\Omega_0/da$ with in-plane lattice parameter a. For several layered hexagonal materials related to NbSe$_2$, including MoS$_2$, boron nitride, and graphite, the Grüneisen parameter is of order unity [28,29]. This suggests that a 0.1% anisotropic phonon energy shift also corresponds to changes of order 0.1% in the interatomic distances.

The transition temperature into the $1Q$ phase increases with uniaxial strain, as the breaking of threefold rotational symmetry stabilizes $1Q$ order. The rates of increase at positive and negative strain differ because, as indicated in Fig. 1(d), the atomic displacements stabilizing the $1Q$ phase are proportional to σ at positive strain, when the CDW order develops along the strain direction, but proportional to $-\sigma/2$ for negative strain, with CDW order at an angle of $2\pi/3$ to the direction of applied strain. We found the $2Q$ state, with two

CDWs at $\pm 2\pi/3$ to the strain direction, to have higher free energy than either the $1Q$ or the $3Q$ state within the range of parameters relevant to NbSe$_2$ [30].

At T_{MMA} and zero strain, the system orders into a $3Q$ geometry via a weakly first-order transition. Within the MMA, phonon fluctuations renormalize the generalized susceptibility, yielding a decreased range of stability for the $3Q$ state as compared to the RPA. Application of just under 0.1% strain then stabilizes the $1Q$ CDW, in agreement with STM findings of a $1Q$ phase in regions with an upper-bound uniaxial strain of about 0.45% [12]. We predict this $1Q$ order to also be stabilized in the bulk upon application of uniaxial pressure to the entire sample.

Conclusions. We compared the stability of proximate $1Q$- and $3Q$-ordered CDW phases in niobium diselenide using a Landau free energy expansion, based on a tight-binding model that was previously shown to capture all of the various known properties of the zero-strain, $3Q$-ordered phase [13]. By comparing the model's phase diagram within the RPA and MMA, it is found that phonon fluctuations, present in the latter, suppress long-range order and lead to the formation of a pseudogap regime between T_{RPA} and T_{MMA} in which the order parameter has a nonzero local magnitude but no long-range phase coherence. Both the pseudogap and CDW phases are shown to have a $3Q$ geometry, but it takes only of order 0.1% uniaxial strain to induce a $1Q$ geometry, in agreement with suggestions that the $1Q$ state seen in STM is stabilized by surface-layer distortions causing local strain [12]. We propose that the bulk quantum phase transition between the different ordering geometries can be accessed by the application of comparable amounts of bulk uniaxial strain.

The free energy expression shows that while, in principle, the $3Q$ phase transition can be either first or second order, any would-be second-order transition is preempted by a weakly first-order transition. We found that the $3Q$ phase at low strain is of this weakly first-order form, in agreement with previous experimental and theoretical studies [26,30–35], while the transition from disorder to the strained 1Q phase is second order.

The CDW wave vector $\mathbf{Q}_{\mathrm{CDW}}$ is dictated by the location of the maximum in the momentum-dependent generalized susceptibility χ, implying that within the short-range-ordered domains of the pseudogap, $\mathbf{Q}_{\mathrm{CDW}}$ can be tracked by the peak in χ between T_{MMA} and T_{RPA}. As temperature increases within the pseudogap, the momentum dependence of the electron-phonon coupling increasingly dominates the bare electronic susceptibility in determining the shape of χ, resulting in a decrease of the CDW wave vector within the locally fluctuating regions. This complements recent experimental work in which a nonmonotonic evolution of the CDW wave vector was found within the ordered state itself [14].

The situation in NbSe$_2$ recalls that in the layered high-temperature superconductors, which exhibit both charge order [36–39]—believed to be close to the phase boundary between the $1Q$ and $2Q$ geometries supported by their square lattices [3,6]—and pseudogaps characterized by some form of fluctuating local order [2–5,40]. Contrary to the high-T_c case, the underlying physics giving rise to these features in NbSe$_2$ is well understood [13]. The interplay of the CDW geometries with external parameters such as applied uniaxial stress may now be used as a test case from which to consider the geometries of charge-ordered states more generally, and may thus shed some light on the case of the high-T_c superconductors.

[1] G. Grüner, Rev. Mod. Phys. **60**, 1129 (1988).

[2] S. A. Kivelson, I. P. Bindloss, E. Fradkin, V. Oganesyan, J. M. Tranquada, A. Kapitulnik, and C. Howald, Rev. Mod. Phys. **75**, 1201 (2003).

[3] A. Melikyan and M. R. Norman, Phys. Rev. B **89**, 024507 (2014).

[4] J. A. Robertson, S. A. Kivelson, E. Fradkin, A. C. Fang, and A. Kapitulnik, Phys. Rev. B **74**, 134507 (2006).

[5] K. Seo, H.-D. Chen, and J. Hu, Phys. Rev. B **76**, 020511 (2007).

[6] R. Comin, R. Sutarto, E. H. da Silva Neto, L. Chauviere, R. Liang, W. N. Hardy, D. A. Bonn, F. He, G. A. Sawatzky, and A. Damascelli, Science **347**, 1335 (2015).

[7] J. A. Wilson, F. J. Di Salvo, and S. Mahajan, Phys. Rev. Lett. **32**, 882 (1974).

[8] K. Rossnagel, O. Seifarth, L. Kipp, M. Skibowski, D. Voß, P. Krüger, A. Mazur, and J. Pollmann, Phys. Rev. B **64**, 235119 (2001).

[9] F. Weber, S. Rosenkranz, J.-P. Castellan, R. Osborn, R. Hott, R. Heid, K.-P. Bohnen, T. Egami, A. H. Said, and D. Reznik, Phys. Rev. Lett. **107**, 107403 (2011).

[10] F. Weber, R. Hott, R. Heid, K.-P. Bohnen, S. Rosenkranz, J.-P. Castellan, R. Osborn, A. H. Said, B. M. Leu, and D. Reznik, Phys. Rev. B **87**, 245111 (2013).

[11] C. J. Arguello, S. P. Chockalingam, E. P. Rosenthal, L. Zhao, C. Gutiérrez, J. H. Kang, W. C. Chung, R. M. Fernandes, S. Jia, A. J. Millis, R. J. Cava, and A. N. Pasupathy, Phys. Rev. B **89**, 235115 (2014).

[12] A. Soumyanarayanan, M. M. Yee, Y. He, J. van Wezel, D. J. Rahn, K. Rossnagel, E. W. Hudson, M. R. Norman, and J. E. Hoffman, Proc. Natl. Acad. Sci. USA **110**, 1623 (2013).

[13] F. Flicker and J. van Wezel, Nat. Commun. **6**, 7034 (2015).

[14] Y. Feng, J. van Wezel, J. Wang, F. Flicker, D. M. Silevitch, P. B. Littlewood, and T. F. Rosenbaum, Nat. Phys. **11**, 865 (2015).

[15] N. J. Doran, D. J. Titterington, B. Ricco, and G. Wexler, J. Phys. C: Solid State Phys. **11**, 685 (1978).

[16] N. J. Doran, J. Phys. C: Solid State Phys. **11**, L959 (1978).

[17] C. M. Varma, E. I. Blount, P. Vashishta, and W. Weber, Phys. Rev. B **19**, 6130 (1979).

[18] S. V. Borisenko, A. A. Kordyuk, V. B. Zabolotnyy, D. S. Inosov, D. Evtushinsky, B. Büchner, A. N. Yaresko, A. Varykhalov, R. Follath, W. Eberhardt, L. Patthey, and H. Berger, Phys. Rev. Lett. **102**, 166402 (2009).

[19] D. J. Rahn, S. Hellmann, M. Kalläne, C. Sohrt, T. K. Kim, L. Kipp, and K. Rossnagel, Phys. Rev. B **85**, 224532 (2012).

[20] A. I. Larkin and S. A. Pikin, Sov. Phys. JETP **29**, 891 (1969).

[21] C. M. Varma and W. Weber, Phys. Rev. Lett. **39**, 1094 (1977).

[22] W. L. McMillan, Phys. Rev. B **16**, 643 (1977).

[23] J. E. Inglesfield, J. Phys. C: Solid State Phys. **13**, 17 (1980).

[24] H. Yoshiyama, Y. Takaoka, N. Suzuki, and K. Motizuki, J. Phys. C: Solid State Phys. **19**, 5591 (1986).

[25] C. M. Varma and A. L. Simons, Phys. Rev. Lett. **51**, 138 (1983).

[26] W. L. McMillan, Phys. Rev. B **12**, 1187 (1975).

[27] U. Chatterjee, J. Zhao, M. Iavarone, R. Di Capua, J. P. Castellan, G. Karapetrov, C. D. Malliakas, M. G. Kanatzidis, H. Claus, J. P. C. Ruff, F. Weber, J. van Wezel, J. C. Campuzano, R. Osborn, M. Randeria, N. Trivedi, M. R. Norman, and S. Rosenkranz, Nat. Commun. **6**, 6313 (2015).

[28] H. J. Conley, B. Wang, J. I. Ziegler, R. F. Haglund, S. T. Pantelides, and K. I. Bolotin, Nano Lett. **13**, 3626 (2013).

[29] N. Mounet and N. Marzari, Phys. Rev. B **71**, 205214 (2005).

[30] D. E. Moncton, J. D. Axe, and F. J. DiSalvo, Phys. Rev. B **16**, 801 (1977).

[31] W. L. McMillan, Phys. Rev. B **14**, 1496 (1976).

[32] W. L. McMillan, Phys. Rev. B **16**, 4655 (1977).

[33] D. E. Moncton, J. D. Axe, and F. J. DiSalvo, Phys. Rev. Lett. **34**, 734 (1975).

[34] J. Harper, T. Geballe, and F. D. Salvo, Phys. Lett. A **54**, 27 (1975).

[35] T. M. Rice, in *Festkörperprobleme 20*, edited by J. Treusch (Springer, Berlin, 1980), pp. 393–411.

[36] V. J. Emery, S. A. Kivelson, and J. M. Tranquada, Proc. Natl. Acad. Sci. USA **96**, 8814 (1999).

[37] R. E. Walstedt, T. E. Mason, G. Aeppli, S. M. Hayden, and H. A. Mook, Phys. Rev. B **84**, 024530 (2011).

[38] J. Chang, E. Blackburn, A. T. Holmes, B. C. N, J. Larsen, J. Mesot, R. Liang, D. A. Bonn, W. N. Hardy, A. Watenphul, M. v. Zimmermann, E. M. Forgan, and S. M. Hayden, Nat. Phys. **8**, 871 (2012).

[39] G. Ghiringhelli, M. L. Tacon, M. Minola, S. Blanco-Canosa, C. Mazzoli, N. B. Brookes, G. M. D. Luca, A. Frano, D. G. Hawthorn, F. He, T. Loew, M. M. Sala, D. C. Peets, M. Salluzzo, E. Schierle, R. Sutarto, G. A. Sawatzky, E. Weschke, B. Keimer, and L. Braicovich, Science **337**, 821 (2012).

[40] A. Mesaros, K. Fujita, H. Eisaki, S. Uchida, J. C. Davis, S. Sachdev, J. zaanen, M. J. Lawler, and E.-A. Kim, Science **333**, 426 (2011).